

2010

Performance of Air-to-Water Heat Pump Using 2 Stage Vapor Injection

Younghwan Ko
LG Electronics

Simon Jin
LG Electronics

Samchul Ha
LG Electronics

Jaekeun Lee
School of Mechanical Eng.

Follow this and additional works at: <http://docs.lib.purdue.edu/iracc>

Ko, Younghwan; Jin, Simon; Ha, Samchul; and Lee, Jaekeun, "Performance of Air-to-Water Heat Pump Using 2 Stage Vapor Injection" (2010). *International Refrigeration and Air Conditioning Conference*. Paper 1137.
<http://docs.lib.purdue.edu/iracc/1137>

This document has been made available through Purdue e-Pubs, a service of the Purdue University Libraries. Please contact epubs@purdue.edu for additional information.

Complete proceedings may be acquired in print and on CD-ROM directly from the Ray W. Herrick Laboratories at <https://engineering.purdue.edu/Herrick/Events/orderlit.html>

Performance of Air-to-Water Heat Pump Using 2 Stage Vapor Injection

Younghwan KO^{1*}, Simon JIN², Samcheol HA³, Jaekeun LEE⁴

¹AC R&D lab., Gasan R&D Campus, LG electronics, Republic of Korea
+82-55-260-3860, younghwan.ko@lge.com

²AC R&D lab., Gasan R&D Campus, LG electronics, Republic of Korea
+82-55-260-3860, simon.chin@lge.com

³AC R&D lab., Gasan R&D Campus, LG electronics, Republic of Korea
+82-2-6915-1105, sam.ha@lge.com

⁴School of Mechanical Eng., Pusan National Univ., Republic of Korea
+82-51-510-2455, jklee@pusan.ac.kr

ABSTRACT

On the heat pump system, Vapor injection (VI) compression cycle's superiority over non-injection cycle has been well known. VI system produces the high heating capacity, and its power consumption is less than the non-injection system. Furthermore, the system design of the vapor compression cycle also minimizes the compressor size.

The investigation of VI cycle's influence on the air-to-water heat pump (AWHP) system is presented. At 35°C water temperature, VI AWHP improves 20% heating capacity and 10% COP compared to the conventional AWHP. At 60°C water temperature, VI AWHP improves 48% heating capacity and 12% COP compared to the conventional AWHP. Experimental results are compared at the same compressor displacement volume.

1. INTRODUCTION

Highly efficient heat pump has a great chance of replacing the residential gas or oil boiler system under the CO₂ reduction regulation. Certainly, the highly efficient heat pump requires improving the compressor efficiency since the compressor consumes the most system power.

At low ambient temperatures, the inverter-driven heat pump can provide the additional heating capacity by increasing the refrigerant flow rate. Generally, the compressor maximum operating frequency causes a large discrepancy between the heating thermal load and the system capacity at cold climate conditions. The cold climate condition significantly reduces the system heating capacity at the maximum operating frequency of the inverter compressor due to low evaporating temperature. In this low outdoor temperature, increasing compressor frequency raises the compression ratio at the practical condition due to a suction pressure reduction and a high discharge pressure. The increased compression ratio and the high discharge temperature degrade the oil and the refrigerant, leading the mechanical failure of the compressor elements.

At the cold climate condition, the heat pump system can achieve the high heating capacity by maintaining the proper compression ratio at the high compressor frequency. At the low ambient temperature, the 2 stage vapor compression cycle maintains the proper compression ratio even at the high compressor frequency. The current research investigates AWHP performance applying the vapor injection cycle. Also, the controlling method of vapor injection cycle component is presented.

2. EXPERIMENTAL SETUP AND TEST PROCEDURE

VI system consists of six main components - evaporator, condenser, 2 stage rotary compressor, phase separator, two expansion devices (EEV1, EEV2) and an injection valve (EEV3). The phase separator receives partially-expanded fluid diverted from the first expansion device and injects it into the 2 stage compressor at an intermediate pressure.

As a result, VI system increases the heating capacity because of an added refrigerant from an injection line. Simultaneously, the reduced inlet quality of the evaporator increases the evaporator capacity. The net effect increases the system capacity and reduces the refrigerant flow rate from the evaporator to the compressor suction. Increased capacity also allows system to minimize the compressor size. A brief description of VI cycle configuration is presented here.

Figure 1 shows that the experimental setup was designed to test VI performance. The test setup consists of a compressor and an injection loop. The experimental setup is installed within the test chamber, which controls the temperature and the humidity level. The compressor and injection loop includes a 2 stage compressor, an evaporator, two expansion valves, an injection valve and a phase separator. The capacity and power input was measured at a specified test condition according to EN14511. The refrigerant leaving the phase separator is divided into two lines: one is the main line entering the second expansion device and the other is the injection line entering to connection pipe of a 2 stage compressor.

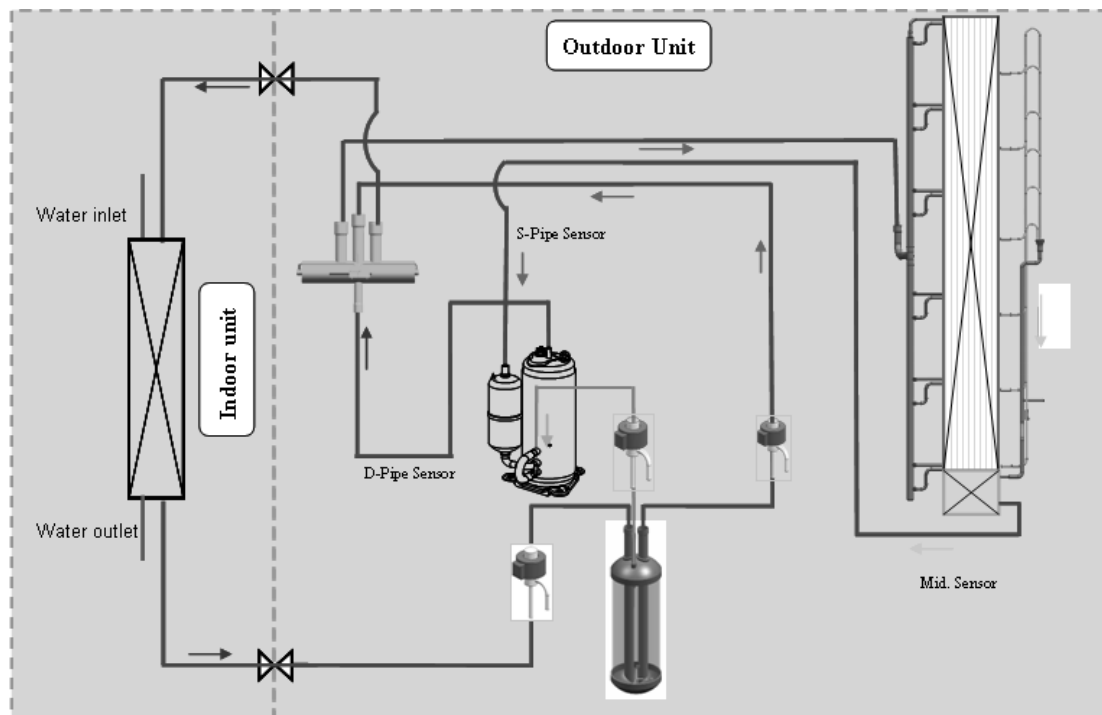


Figure 1 System layout and test apparatus

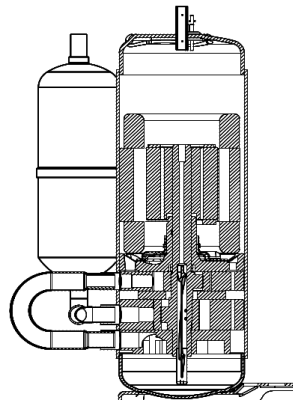


Figure 2 2 stage compressor

Figure 2 shows the schematic of the 2 stage compressor with connection pipe. The compressor is an inverter-driven rotary compressor with a displacement volume of 42.5 cm^3 and built in the volume ratio of 0.63. The vaporized gas is drawn into the accumulator and the suction pipe. The vaporized gas is compressed in the lower cylinder, and then flows into the cycle one by one such as the suction plenum, the connection pipe, and the upper cylinder. The compressor shell is filled with the high-pressure discharge gas, exposed to the discharge port. The compressor is newly developed for a commercial product by precisely machining core components.

A computer data acquisition system monitors temperature, pressure, mass flow rate, and power input in the test loop. The refrigerant flow rate passing through the injection loop is measured by a Coriolis type mass flow meter with an estimated accuracy of $\pm 0.2\%$. The compressor power input is monitored by a digital power meter with an uncertainty of $\pm 0.1\%$. The pressure transducer calibrated with a standard dead weight tester measures the compressor suction and the discharge pressure. The estimated accuracy of the pressure measurement is $\pm 0.13\%$ of full scale (4.5 MPa). All temperatures in the system are monitored using T-type thermocouples. The accuracy of the temperature measurements is estimated at $\pm 0.2^\circ\text{C}$.

Based on the measured temperature, the pressure, the mass flow rate and the power input data; the following equations represent how to compute the heating capacity and the coefficients of performance (COP).

$$Q = m_w \times C_p \times (T_{w_in} - T_{w_out}) \quad (1)$$

$$P = P_{\text{Power}} + P_{\text{fans}} + P_{\text{pump}} \quad (2)$$

$$\text{COP} = Q / P \quad (3)$$

where C_p shows the average specific value calculated by the water temperature measurement. Table 1 summarizes the experimental parameter uncertainty. Refrigerant R410A is a working fluid and PVE is utilized as a lubricant.

Table 1 Uncertainties

Parameters	Uncertainty
Temperature(T-type thermocouple)	$\pm 0.2^\circ\text{C}$
Pressure(Pressure transducer)	$\pm 5.8\text{kPa}$
Mass flow rate(Coriolis type)	$\pm 0.2\%$ of reading
Power(Yokogawa)	$\pm 0.1\%$ of rated output

3. RESULTS AND DISCUSSION

3.1 2 stage compressor performance

2 stage compressor performance test is carried out under ARI condition: the suction and the discharge absolute pressures of 0.995 and 3.381 MPa, the suction superheat of 11.1 °C, the subcooling of 8.3 °C and the ambient temperature of 35 °C. The compressor frequency is increased from 30 Hz to 90 Hz by 30 Hz. Test data were taken at steady state with a varied operating condition.

Figure 3 shows the EER and the capacity as a function of the frequency, compared by the normal twin compressor of the non-injection condition. M-company provides the approval sheet of the general twin compressor. Since the capacity was measured at the constant subcooling and superheat, the enthalpy difference across the evaporator remained nearly constant. Therefore, the capacity represents the discharge mass flow rate at the non-injection condition.

The capacity effects of 2-staged compression at low frequency are negligible but the EER increase by 7.1 % as compared to the twin compressor. The capacity at high frequency is increased by 3.8%, while the EER decreased by 4.8 %. Thus, a 2 stage compressor consumes the less power at low frequency and maintains the high volumetric efficiency at high frequency.

3.2 Vapor injection effects

Figure 4 shows the effects of VI on heating capacity with EEV3 opening at low ambient temperature. Heating capacity is linearly increased with EEV3 opening and saturated on some enough opening. Generally, the optimum EEV opening depends on the outdoor temperature and the compressor frequency. The big difference between the condenser pressure and the suction pressure is caused by the higher frequency at lower outdoor temperature. The pressure difference between the condenser and the suction drives the injection refrigerant flow. The heating capacity increment increases the condenser mass flow rate. The larger pressure difference between the injection port in the 2 stage compressor and the phase separator drives the rise of the condenser mass flow rate. Therefore, the EEV opening becomes larger because of the pressure difference rise.

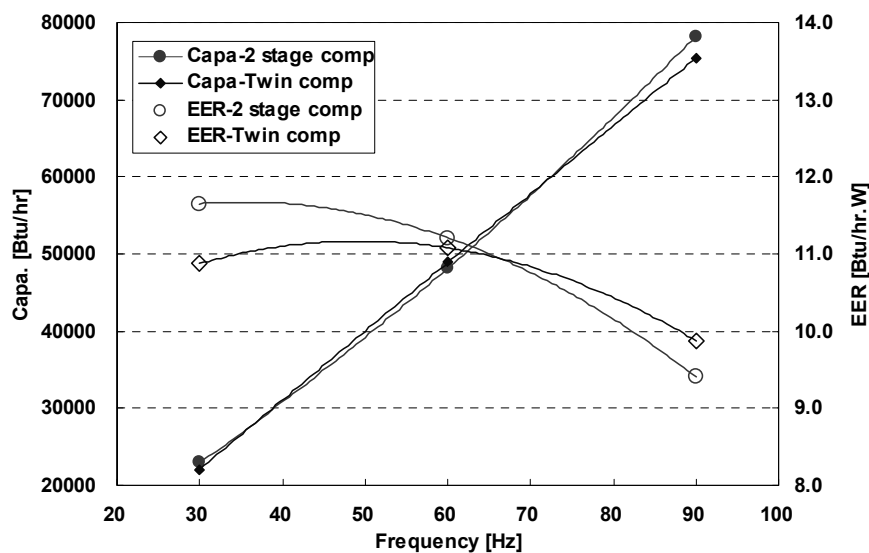


Figure 3 2 stage compressor performance

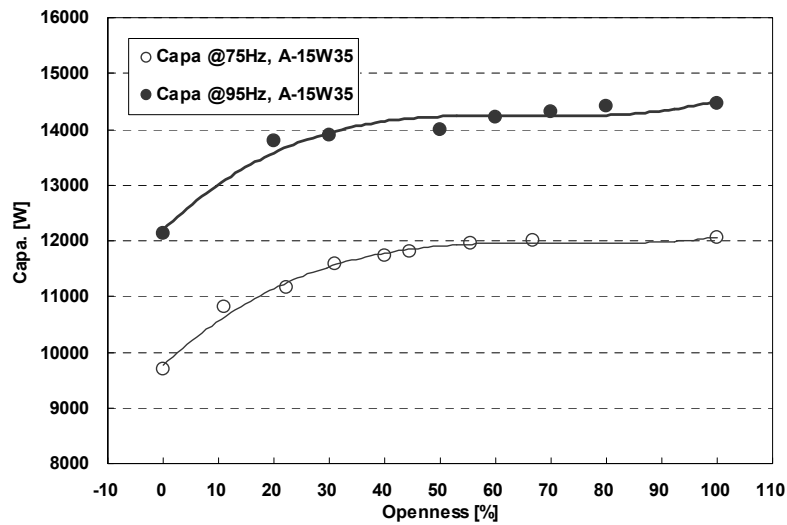


Figure 4 Heating capacity increase by vapor injection with EEV openness

Figure 5 and Figure 6 present the pressure variation respect to the non-injection condition as a function of the frequency. The pressure of phase separator is nearly constant with increasing frequency at a given non-injection condition. But the phase separator pressure with EEV3 opening drops to the equilibrium between the phase separator and the connection pipe. On the other hand, the connection pipe pressure with EEV3 opening slightly increases because the mechanical loss becomes smaller with the injection mass flow rate rise.

The suction pressure is nearly constant regardless of the injection or the non-injection condition. The discharge pressure with the non-injection slightly increases, but the discharge pressure with the injection linearly increases by 228kPa. As a result, heating capacity increase and the condenser mass flow rate rises.

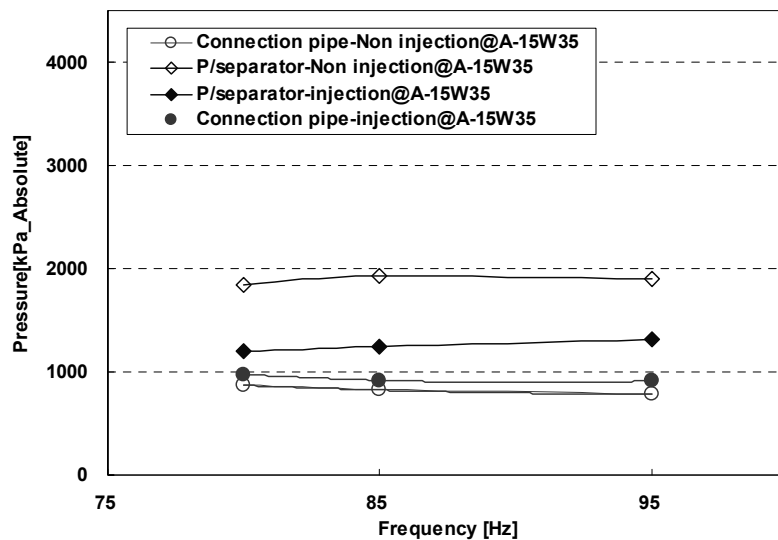


Figure 5 Pressure variations with injection and non-injection

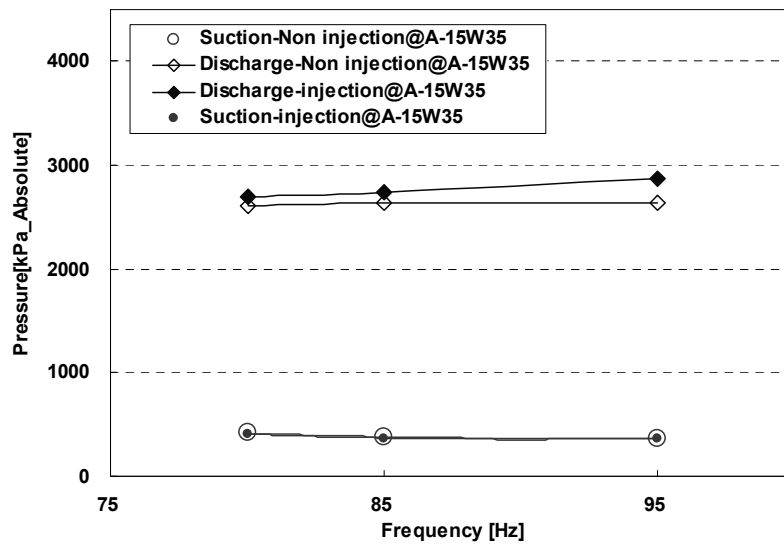


Figure 6 Pressure variations with injection and non-injection

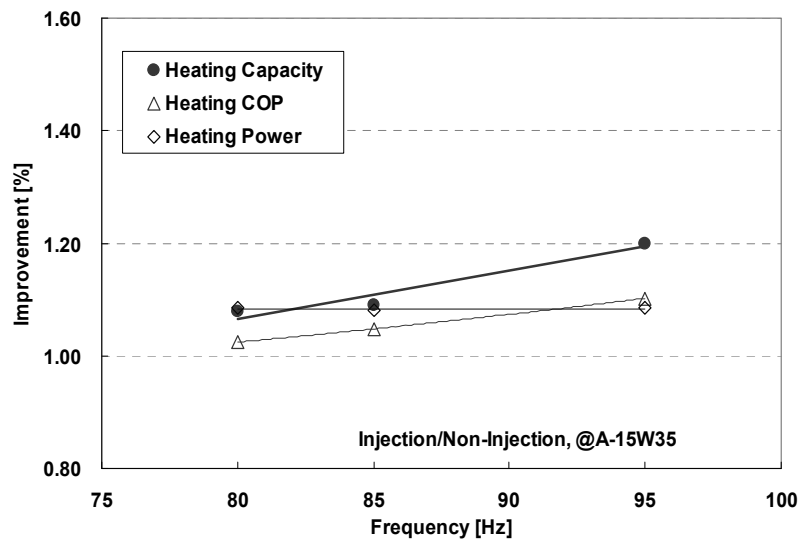


Figure 7 Heating performance effects by vapor injection

Figure 7 shows the capacity as a function of the frequency, normalized by the comparable capacity for the non-injection condition. The normalized capacity represents the ratio of injection mass flow rate at the injection condition to that of the non-injection case. The normalized capacity of all injection condition rises with increasing the frequency because the mass flow rate increment in condenser becomes larger as compared to the non-injection condition. For the frequency of 80 Hz, the capacities with vapor injection increase by 7.5% as compared to the non-injection case, while for the frequency of 95 Hz, the capacities increase by 20%. But the normalized power is constant. The normalized COP becomes higher at high frequency with the increased injection.

3.3 Vapor injection effects with water temperature and outdoor temperature

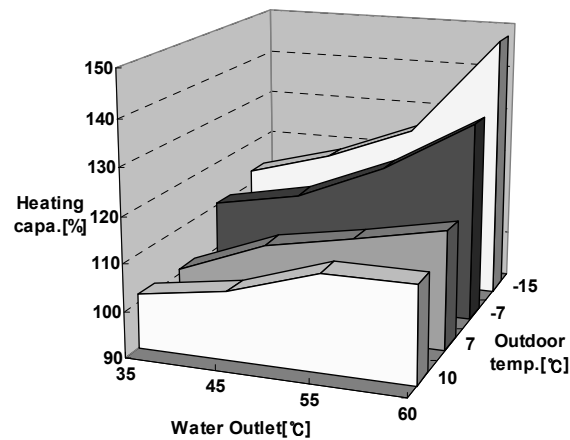


Figure 8 Heating capacities by vapor injection with water temperature and outdoor temperature

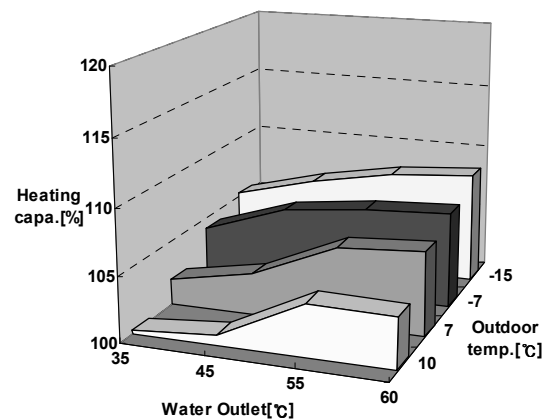


Figure 9 Heating COPs by vapor injection with water temperature and outdoor temperature

Generally, the injection effects on the heating capacity and COP depend on the operating frequency, the pressure difference between evaporator and condenser. The lower outdoor temperature and the higher water temperature and frequency, the higher injection effects on heating capacity and COP. The injection mass flow rate may vary respect to the water temperature and the outdoor temperature due to the pressure difference change in the compression pocket. All experimental results are tested according to EN14511 in order to investigate the injection effect.

The experimental results of heating capacity obtained maintaining the outdoor temperature and the water temperature are compared to the non injection results. Figure 8 and Figure 9 presents the heating capacity as a function of the outdoor temperature and the water temperature. 20% heating capacity gain with 10% COP improvement at the 35°C water temperature and 48% heating capacity improvement with 12% COP gain at the 60°C water temperature were found for vapor injection as compared to the non injection conditions.

4. CONCLUSIONS

To investigate the reasonable heating capacity and COP in AWHP, the injection performance study is carried out. The influence of the vapor injection on AWHP is presented with varying the compressor frequency, the injection pressure and the injection mass flow rate. It is observed that the vapor injection at the high frequency and the low ambient temperature shows the drastic improvement of heating capacity and COP. However, the power consumption rise by function of the compressor frequency shows nearly constant.

The large injection pressure difference between the phase separator and the connection pipe drives the injection mass flow rate leading the power input increment. An optimum EEV opening of injection valve should be selected to provide appropriate system performance.

NOMENCLATURE

AWHP	air-to-water heat pump	(–)	Subscripts	
Capa	capacity	(–)	Comp	compressor
COP	coefficient of performance	(–)	Cond	condenser
C_p	specific heat at constant pressure	(J/kgK)	Evap	evaporator
EEV	electronic expansion valve	(–)	In	inlet
DB	dry bulb temperature	(°C)	Out	outlet
H	enthalpy	(kJ/kg)	W	water
M	mass-flow-rate	(kg/s)		
T	temperature	(°C)		
Q	heat transfer rate	(W)		
P	work	(W)		
W	water	(–)		
WB	wet bulb temperature	(°C)		

REFERENCES

- P.A. Domanski, D.A. Didion, J.P. Doyle, Evaluation of suction line/ liquid-line heat exchange in the refrigeration cycle, *International Journal of Refrigeration* 17 (1994) 487e493.
- C. Aprea, M. Ascani, F. Rossi, A criterion for predicting the possible advantage of adopting a suction/liquid heat exchanger in refrigerating system, *Applied Thermal Engineering* 19 (1999) 329e336.
- ASHRAE Guideline 2, Engineering Analysis of Experimental Data, ASHRAE, Atlanta (GA), 1986.
- Arora, C. P., Dhar, P. L. Optimization of multi-stage refrigerant compressors, *Proc. 13th Int. Cong. of Refrigeration, IIR, Paris (1971) Vol. 2, 693-700*
- Prasad, M. Optimum interstage pressure for 2-stage refrigeration system, *ASHRAE Journal* (1981) 23 (1), 58-60
- Zubair, S. M., Khan, S. H. On optimum inter-stage pressure for two-stage and mechanical-subcooling vapor-compression refrigeration cycles, *Trans. ASME, J. Solar Energy Engng* (1995) 117 (1), 64-66
- London, A. L. Economics and the second-law: an engineering view and methodology, *Int. J. Heat Mass Transfer* (1982) 26 (6), 743-751
- S.M. Zubair, M.Yaqub and S.H.Khan, Second-law-based thermodynamic analysis of two-stage and mechanical-subcooling refrigeration cycles, *International Journal of Refrigeration*, 19, 506-516, 1996.
- S.S. Bertsch, E.A. Groll, Air to Water Heat Pump for Low Temperature Climates, 8th International Energy Agency Heat Pump Conference, Las Vegas, NV, CD-ROM, 2005.

ACKNOWLEDGEMENT

This work was supported by Air Conditioning Research and Development Laboratory in LG Electronics Inc.